

V. Yu. Kashtan,  
orcid.org/0000-0002-0395-5895,  
V. V. Hnatushenko\*,  
orcid.org/0000-0003-3140-3788

Dnipro University of Technology, Dnipro, Ukraine  
\* Corresponding author e-mail: [vygnat@ukr.net](mailto:vygnat@ukr.net)

## INTELLIGENT TECHNOLOGY FOR LAND COVER MONITORING DUE TO AMBER MINING ON OPTICAL SATELLITE IMAGES

**Purpose.** This article proposes to develop an intelligent technology for detecting land cover changes due to amber mining based on Sentinel-2 optical satellite images.

**Methodology.** The presented intelligent technology combines methods of geometric and radiometric correction, the Dark Object Subtraction algorithm, a hybrid architecture of convolutional neural networks (CNN + EfficientNet-Edge), and an algorithm for detecting changes over time based on the symmetric difference of changed pixels, which ensures high accuracy and efficiency in the process of analysing land cover changes.

**Findings.** The effectiveness of the proposed technology was assessed using the F1-score, Recall, Precision, and Accuracy metrics. The values of the recall and F1-score metrics (92 %) confirm the ability of the system to detect the boundaries of land cover disturbance zones accurately. In addition, the accuracy (94 %), recall (90 %), and overall accuracy (93 %) confirm the ability of the model to effectively classify both mining-impacted areas and areas without signs of anthropogenic interference with a minimum number of errors. The low value of land cover change segmentation error (4.7 %) indicates the high quality of spatial interpretation of the results.

**Originality.** The paper proposes a comprehensive use of convolutional neural networks with the EfficientNet-Edge architecture to detect land cover changes due to amber mining. This approach overcomes the limitations of traditional feedforward neural networks associated with problems of incorrect initialization and suboptimal distribution of weight coefficients. In particular, a comprehensive use of two feature processing levels is proposed: the first one processes simple texture features obtained using average pooling in the CNN architecture, and the second one processes spectral features formed from a 4D tensor at the last convolutional layer of EfficientNet-Edge. This helps to overcome the instability of the training process and improve the ability of the model to detect land cover changes caused by hydromechanical amber mining accurately. An annotation of areas resulting from amber mining and areas without signs of anthropogenic interference was developed.

**Practical value.** The developed technology has practical value for determining changes in the land cover caused by hydromechanical extraction of amber. The theoretical results obtained allow for an effective assessment of the scale of changes and facilitate informed management decisions in environmental protection.

**Keywords:** *land cover change map, spectral features, textural features, EfficientNet-Edge, deep learning, convolutional neural networks, optical satellite images*

**Introduction.** A variety of factors can cause land cover disturbances, both natural: floods [1, 2], fires [3, 4], droughts; and anthropogenic ones: deforestation [5], urbanization, which poses a serious threat to the ecological stability of the planet. Such changes significantly affect the functioning of the ecosystem by altering hydrological, biogeochemical, and climatic processes. Given global trends, such as increased extreme weather events and the active expansion of urbanized areas, land cover disturbances are becoming more common and can have significant consequences for ecosystems and humanity.

The illegal amber extraction in the northwestern region of Ukrainian Polissya (Volyn, Rivne, Zhytomyr, and Kyiv oblasts) is one of the environmental problems of our time. Intensive and uncontrolled mining activities

lead to catastrophic changes in the land cover, which have long-term consequences for natural ecosystems. Disruption of the relief structure and landscapes, degradation of soil cover, changes in hydrological conditions, and destruction of forest ecosystems are the consequences of this phenomenon. The emergence of quarries and trenches on the land cover changes the natural relief, leading to the fragmentation of landscapes and the loss of their aesthetic value. The destruction of hills, ravines, and gullies disrupt natural water runoff, contributing to soil erosion. Deforestation for access to amber deposits also has negative environmental impacts, including loss of biodiversity, changes in microclimate, and increased erosion.

Land cover monitoring includes identifying and assessing changes on the Earth's surface using multitem-

poral or multispectral images. Optical images have been widely used for land cover change monitoring [6]. The high spatial resolution of optical images allows for a detailed analysis of the morphological features of the Earth's surface, and the spectral information, including visible and infrared bands, makes it possible to assess both structural and ecosystem changes [7].

For instance, multispectral imagery is available from Landsat [4, 8], Sentinel-2 [9], QuickBird, SPOT, and high-resolution satellite series [10]. Each of the above satellite systems provides data with different spatial, spectral, and temporal resolution characteristics and data availability for a specific region, which allows for optimizing the choice of data source according to the particular requirements of the study.

**Literature review.** Several methods have been developed in recent years to detect land cover changes using optical satellite imagery. These methods can be classified according to several criteria: time series-based; feature extraction, which defines the approach to identifying and highlighting key land cover characteristics; application of a priori information to improve the accuracy of change detection and process modeling; type of satellite data, which determines the platform and sensor used (optical [11, 12] or radar images [13]); structural object detection, which includes technologies for classifying objects such as buildings, roads or infrastructure elements; detection systems based on machine learning, classification, or segmentation algorithms to detect changes.

Time series-based methods include using multi-temporal images to monitor land cover changes. The authors in [14] proposed a new UTAE architecture that improves existing models, scales better in terms of the number of parameters, and uses long-term temporal information to detect semantic changes using satellite image time series (SITS-SCD).

Traditional detecting methods for structural objects are classified into two main categories: pixel-oriented and object-oriented. Pixel-oriented methods analyze satellite images at the level of individual pixels, determining changes in their spectral characteristics [15]. Previous approaches involved the use of simple algebraic operations and threshold segmentation. At the same time, modern methods are based on more complex algorithms, such as principal component analysis and morphological transformations. Despite the simplicity and computational efficiency of pixel-based methods, they have limitations. In particular, their high sensitivity to noise and atmospheric influences [16] leads to data distortion. In addition, these methods consider each pixel separately, without considering spatial information and dependencies between neighboring pixels, which leads to the formation of "salt and pepper" noise. It reduces the accuracy of detecting land cover changes, especially over large areas. Object-based change detection methods analyze objects using their geometric, texture, spectral, and spatial features [17]. The procedure involves segmenting images into objects with similar attributes, after which a comparative analysis of the features of the corresponding objects at different time points is performed to detect changes.

Object-oriented methods demonstrate advantages in reducing noise-induced classification and increasing

accuracy in detecting changes. The effectiveness of object-oriented methods depends on the correct choice of object segmentation parameters [18]. In [19], an approach to detecting and assessing land cover changes caused by illegal amber mining is presented based on time segmentation of the normalized burning rate and estimating carbon losses in a limited area. Although effective in detecting changes in forest cover, the proposed method has limitations. Namely, the delta-normalized burning rate focused on detecting sudden disturbances does not correctly reflect the complex recovery processes and multidirectional changes in ecosystems disturbed by illegal amber mining. The authors in [20] propose an approach to monitoring land cover disturbances caused by illegal amber mining using four-band Planet Labs PBC satellite images over a 40-hectare area. While the images provide high spatial detail, their limited spectral resolution makes it difficult to accurately determine the condition of vegetation and soil compared to multispectral imagery. In addition, the limited detail in geospatial analysis methods, such as image classification, change detection algorithms, and geospatial models, makes it difficult to assess the accuracy and reliability of the results. In the paper [21], the authors proposed a technique for monitoring land disturbance by merging Landsat and Sentinel satellite data, which includes classification and temperature analysis to identify areas disturbed by illegal amber mining. However, the method has limitations; namely, during the classification step, there is a risk of including areas disturbed by amber mining and dumps created by other anthropogenic activities, such as deforestation or agricultural activities, in the disturbance zone. The author's work [22] proposed a technology for the automated detection of illegal amber mining using Landsat 7 (ETM) and Landsat 8 (OLI) satellite images. The paper comprehensively uses techniques such as data dimensionality reduction using the principal component analysis (PCA) method, creating a different image to compare two images simultaneously, threshold binarization, morphological filtering, and vectorization. The proposed technology demonstrates effectiveness for detecting amber mining areas on Landsat images but has limitations when applied to Sentinel-2 images. PCA for Sentinel-2 images is less effective due to their high spectral resolution, making extracting informative principal components necessary for detecting land cover changes challenging. Threshold binarization and morphological filtering on high-resolution images do not always give correct results, as such images are characterized by high detail and texture complexity, which makes it challenging to classify land cover changes correctly. Vectorization on Sentinel-2 imagery also leads to inaccuracies in determining the boundaries of disturbed areas, as the size of objects may be smaller than the pixel resolution, which requires additional adjustments to detect disturbances correctly.

Nowadays, deep learning technologies are the basis for most modern monitoring of changes in the earth's surface [23]. The primary approach is to use an ensemble of parallel classifiers that perform an identical task but differ in training parameters. For example, combining the results of classifiers built based on convolutional neural networks (CNNs) with different sizes of convolutional filters (e.g.,  $3 \times 3$ ,  $5 \times 5$ , or  $7 \times 7$ ) is widely used

[24]. Another promising area is detecting changes based on multiscale feature analysis, including texture and morphological features. Multiscale object-oriented methods are also used, in which variability is achieved by changing the scale of objects using morphological operations or segmentation algorithms. Ensemble learning methods, which combine the results of several classifiers to form a final solution, effectively improve the accuracy of monitoring changes in the earth's surface [25]. Due to the cross-compensation of errors of individual classifiers, this approach reduces the overall error and increases the reliability of the results.

Ecological monitoring of areas affected by illegal amber mining is essential for assessing and minimizing adverse environmental impacts. One of the main problems is the different image formation mechanisms caused by using various types of satellite sensors. It results in different image characteristics, making it difficult to merge them from other sources into a single data set necessary for accurately monitoring land cover disturbances caused by anthropogenic factors [26]. Differences in the acquisition angle and image resolution make it essential to use adapted algorithms to process such data [27]. Moreover, although high-resolution images contain more details about objects on the Earth's surface, they pose significant difficulties in analysis. The increased heterogeneity of the images, the variability of object sizes, and the presence of scattering and speckle noise variations significantly complicate the interpretation and classification of the data. The last significant problem is the lack of publicly available datasets generated from Sentinel-2 optical imagery for monitoring land cover changes due to amber mining. Developing new machine learning algorithms is necessary due to the annotation complexity and the high cost of manual processing of large amounts of data [28].

Thus, traditional monitoring methods are often time-consuming and do not allow fast-tracking of changes over large areas. To successfully perform such assessments, it is necessary to use new monitoring methods, particularly remote sensing, allowing for practical analysis of large areas and detection of changes in the environmental state of the environment. To automatically detect and classify land cover disturbances based on satellite imagery, it is advisable to use convolutional neural networks (CNN), which increase the accuracy of detecting changes and minimize the influence of the human factor.

**Purpose.** This paper aims to develop intelligent technology for detecting land cover changes due to amber mining based on Sentinel-2 optical satellite images. To improve the segmentation, classification, and time-based land cover disturbance detection resulting from water pumping, we propose integrating convolutional neural networks with the EfficientNet-Edge architecture to monitor the land cover changes due to amber mining.

In this work, to achieve the aim, the following tasks were formulated and solved:

- to develop a methodology for pre-processing Sentinel-2 satellite images, including geometric and radiometric correction, Dark Object Subtraction algorithm to remove atmospheric artifacts on optical satellite images;

- to create training sets that include areas with amber mining and non-amber mining;

- to develop and optimize a hybrid convolutional neural network architecture (CNN + EfficientNet-Edge) for detailed segmentation and classification of land cover changes due to amber mining;

- to develop an algorithm for temporal detection of land cover changes based on the symmetric difference of changed pixel sets using a convolutional neural network;

- to develop a color map of land cover changes algorithm based on the pixel classification obtained using a convolutional neural network to improve the spatial interpretation of the results;

- to test the effectiveness of the proposed technology on real datasets covering regions that have changed due to amber mining as a result of water pumping;

- to evaluate and compare the proposed technology with traditional methods, evaluating metrics such as F1-score, precision, recall, and accuracy.

**Methods.** In this study, we propose using a hybrid architecture of convolutional neural networks CNN + EfficientNet-Edge to monitor land cover changes due to amber mining based on the Sentinel-2 optical satellite data analysis. The block diagram of the proposed intelligent information system is shown in Fig. 1.

Land cover changes monitoring is based on the use of Sentinel-2 satellite images containing spectral channels

$$I_1 = \{I_{1CA}, I_{1R}, I_{1G}, I_{1B}, I_{1NIR}, I_{1VRE}, I_{1WV}, I_{1SWI}\},$$

where  $I_{1CA}$  is Coastal and Aerosol band;  $I_{1R}$  is Red band;  $I_{1G}$  is Green band;  $I_{1B}$  is Blue band;  $I_{1NIR}$  is Near Infrared band;  $I_{1VRE}$  is Vegetation red edge band;  $I_{1WV}$  is Water vapour band;  $I_{1SWI}$  is Short Wave Infrared band.

Each pixel in the  $I_n$  is represented by a reflectance value  $R(x, y)$ , normalized to the range [0, 1] in the Sentinel-2 L2A output images.

The second step involves preliminary data processing, including geometric and radiometric correction. The geometric correction eliminates distortion from sensor system errors and satellite orbital dynamics. The geometric correction process is determined through the projection operator, which performs a projective transformation

$$G(T, p) = h^{-1}(T \cdot h(p)),$$

where  $T \in R^{3 \times 3}$  is the projective transformation matrix;  $p \in R^2$  are image point coordinates.

Suppose we are given a pair of images  $I_1, I_2 \in R^{W \times H \times K}$ , image preprocessing methods  $L_1, L_2$ , image matching method  $M$  and a method for constructing a projective transformation matrix  $R$ .

The result of method  $M$  applied to the results of preprocessing  $I_1, I_2$  is a set of point pairs  $P_0$

$$P_0 = \{(p_1, p_2) \mid p_1, p_2 = M(L_1(I_1), L_2(I_2))\},$$

where  $p_1, p_2$  are coordinates of unique points on the first and second images.

Image matching methods based on key points can produce false point matches, and without additional information, it is impossible to determine which matches are correct. Therefore, false matches must be filtered out.

Suppose  $P_1 \subseteq P_0$  is a set of point pairs filtered with additional information. If no filtering is applied,  $P_1 = P_0$

is assumed. Using these notations, the set of points  $P_1$  can be defined as follows

$$d(p_1, p_2) = \|\text{Pr}(T_1, p_1) - \text{Pr}(T_2, p_2)\|^2;$$

$$P_1 = \{(p_1, p_2) \mid p_1, p_2 \in P_0, d(p_1, p_2) \leq \delta\},$$

where  $\delta$  is an algorithm parameter that sets the maximum allowable deviation between points in real coordinates; the value  $\delta$  is determined a priori, depending on the georeferencing accuracy for specific types of images. In particular, if  $\delta_1$  is the coordinate error of the first type of image, and  $\delta_2$  is the second, then the value is  $\delta = d_1 + d_2$ .

Radiometric correction converts digital  $DN$  values into surface reflections

$$R = \frac{DN \cdot M + A}{\cos(\theta)},$$

where  $M$  is the scale factor;  $A$  is the additive correction;  $\theta$  is the zenith angle of the Sun.

In addition, the Dark Object Subtraction algorithm is used to remove atmospheric artifacts

$$R' = R - R_{atm},$$

where  $R_{atm}$  is the atmospheric component estimated from the darkest pixels.

After pre-processing, a set is formed

$$P = \{(X_i, Y_i)\}_{i=1}^N,$$

where  $X_i$  is image fragment;  $Y_i$  is class designation (0 is Nonamber; 1 is Amber).

For training, validation, and testing of the developed hybrid architecture of convolutional neural networks (CNN + EfficientNet-Edge), a dataset was generated that reflects changes in land cover due to amber mining, which occurs due to water pumping. Creating training samples began with identifying areas with amber mining (the “amber” category) and without signs of anthropogenic intervention (the “non-amber” category). For this purpose, Sentinel-2 optical satellite imagery was used, supplemented by data from open geoinformation resources, such as cadastral maps and aerial photographs. Each site was carefully marked, creating masks that reflect the boundaries of the “amber” and “non-amber” zones.

The collected and annotated images are divided into three primary samples: a training set of  $P_{train}$  70 % of the images, a validation set of  $P_{val}$  15 %, and a test set of  $P_{test}$  15 %.

The next step applies convolutional neural network classification of land cover changes. The input data are images of size  $H \times W \times C$ , where  $H = 64$ ,  $W = 64$ ,  $C = 3$  (RGB channels). Convolutional layers (Conv) use  $3 \times 3$  kernels to detect local features, such as texture characteristics and spectral patterns. Using 64 filters in each convolutional layer allows you to detect various image features, ranging from simple contours to more complex textures. Each convolutional layer calculates

$$F_{i,j}^{(l)} = \sigma \left( \sum_{m=0}^{k-1} \sum_{n=0}^{k-1} W_{m,n}^{(l)} X_{i+m,j+n}^{(l-1)} + b^{(l)} \right),$$

where  $F_{i,j}^{(l)}$  is output activation signal;  $W_{m,n}^{(l)}$  is convolution kernel with size  $k \times k$ ;  $X_{i+m,j+n}^{(l-1)}$  is input image;  $b^{(l)}$  is offset;  $\sigma(x)$  is ReLU activation function

$$\sigma(s) = \max(0, x).$$

After each convolutional layer, a Max Pooling operation with a  $2 \times 2$  kernel is used to reduce the dimensionality of the data. After the first convolutional layer, we get the dimensional features

$$H' \times W' \times C' = 32 \times 32 \times 64.$$

The second convolutional layer (Conv2) uses 128  $3 \times 3$  filters with ReLU activation. After applying Max Pooling ( $2 \times 2$  kernel), the output dimensionality is reduced to

$$H' \times W' \times C' = 16 \times 16 \times 128.$$

Researchers are exploring different approaches to scaling the architecture to improve the efficiency of neural networks. The most common methods include increasing the width of the network (increasing the number of channels in each layer, which allows for the extraction of more local features), the depth of the network (adding more convolutional layers to detect multilevel features), and the resolution of the input image. However, individual scaling of these parameters can lead to inefficient use of resources and increased computational complexity. The method of joint scaling, which is implemented in the EfficientNet architecture, was proposed to achieve an optimal balance between these characteristics. The basic block of the model is the Mobile Bottleneck Convolutional Layer (MBConv), which consists of three main components: the expansion layer increases the number of channels in the hidden layer; Depthwise Convolution processes each channel independently; and the Squeeze-and-Excitation layer adaptively changes the importance of each channel.

In the last convolutional layer, we get a 4D feature tensor

$$Z = f(W_e \times X + b_e),$$

where  $W_e$  is the kernel of the last level convolution of EfficientNet-Edge;  $f$  is a nonlinear activation function.

Thus, using a classical CNN combined with EfficientNet allows for a comprehensive image representation, where CNN effectively detects basic texture features, and EfficientNet detects spectral features.

The combination of features of two architectures is carried out through the concatenation of features

$$F_{concat} = [F_{CNN}, F_e].$$

Next, a fully connected layer and the Softmax function are used to determine classes using the cross-entropy function:

$$\hat{y} = \text{softmax}(W^{(2)}\mathbf{h} + b^{(2)});$$

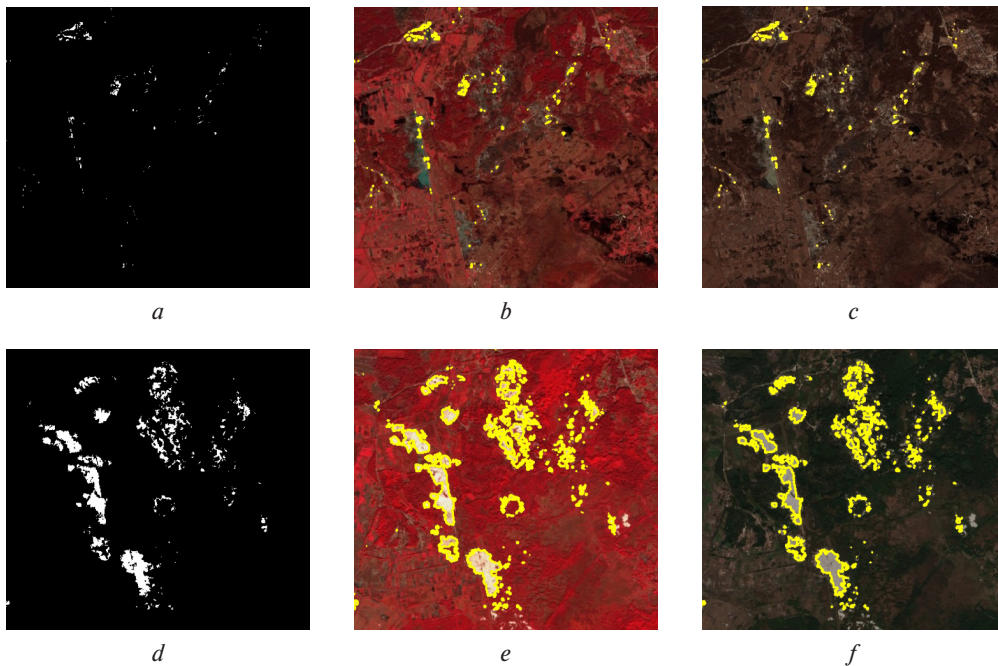
$$\text{softmax}(x)_i = \frac{e^{x_i}}{\sum_j e^{x_j}};$$

$$L = \frac{1}{N} \sum_{i=1}^N (Y_i \log \hat{Y}_i + (1 - Y_i) \log(1 - \hat{Y}_i)).$$

After classification, the resulting image undergoes an additional processing step: the detection of land cover change contours, allowing for better spatial interpretation of the results.

The next step is to detect changes in the land cover over a certain period. For this purpose, the result of a





*A legend:* land cover areas; hydromechanical amber extraction areas; contour of land cover disturbance due to hydromechanical amber mining

*Fig. 2. Sentinel-2 imagery of Rivne region:*

*a – binary mask, 2017; b – pseudo-color representation, 2017; c – True Color representation, 2017; d – binary mask, 2024; e – pseudo-color representation, 2024; f – True Color representation, 2024*

In addition, the mining process destroys the root system of trees, which leads to the destruction of large areas of forest plantations.

To train the neural network, a dataset representing land cover changes in the territory of Ukraine, in particular in the context of amber mining, was created. The images included in this dataset are  $64 \times 64$  pixels obtained from multispectral satellite images. The dataset contains multi-temporal images, which allows the neural network to learn the variable processes caused by amber washing. Thanks to this approach, the model can accurately detect soil degradation, vegetation destruction, and changes in humidity typical of amber mining sites.

The neural network training procedure included 100 iteration epochs. The model was compiled using Adam’s optimizer [29], which adaptively updates network weights based on average gradient values, providing more stable training than the traditional stochastic gradient descent method. The learning rate was set at 0.001, allowing optimal results without significant fluctuations in the training process. The model output is a binary mask, where one class is responsible for land cover changes and the other for the background. Based on this mask, contours are drawn on optical images to clearly define the contours of the altered areas associated with the amber washing process. The softmax activation function was used to normalize the initial values and generate a probability distribution.

The experimental studies compared several deep neural network architectures for detecting land cover changes based on optical images. The models used for the comparison include ResNet50, MobileNet, Inception, NASNet, EfficientNet, and the proposed CNN+ EfficientNet-Edge-based technology.

Metrics were utilized to assess the performance of each model objectively (Table 1) [22]: the F1-score, which combines both precision and recall, is used to evaluate model performance, particularly in cases of class imbalance, i. e., when one category has significantly fewer samples than the other; Accuracy is the percentage of correctly classified samples out of the total number; Recall measures the model’s ability to identify all positive samples in the dataset; Precision represents the proportion of correctly classified positive samples among all those classified as positive by the model.

ResNet50 demonstrated F1-score (0.88), accuracy (0.91), and low recall (0.85), which is vital for detecting changes in images. The MobileNet model has the lowest performance among the compared models: F1-score (0.84), accuracy (0.87), and recall (0.81), which indicates its limited effectiveness for complex monitoring land cover change.

*Table 1*

Quantitative assessments

Model	Metrics			
	F1-score	Accuracy	Recall	Precision
ResNet50	0.88	0.91	0.85	0.90
MobileNet	0.84	0.87	0.81	0.86
Inception	0.86	0.89	0.83	0.87
NASNet	0.89	0.92	0.86	0.91
EfficientNet	0.91	0.93	0.88	0.92
<b>CNN+ EfficientNet-Edge</b>	<b>0.92</b>	<b>0.94</b>	<b>0.90</b>	<b>0.93</b>

The Inception model performed better regarding F1-score (0.86) and accuracy (0.89) but was still inferior to EfficientNet and NASNet in overall performance. The NASNet model achieved high performance, particularly in accuracy (0.92) and F1-score (0.89), but was inferior to EfficientNet.

The CNN + EfficientNet-Edge model proposed in this study showed the highest performance among all models, with F1-score (0.92), precision (0.94), and recall (0.90). This indicates the high efficiency of this technology for monitoring land cover.

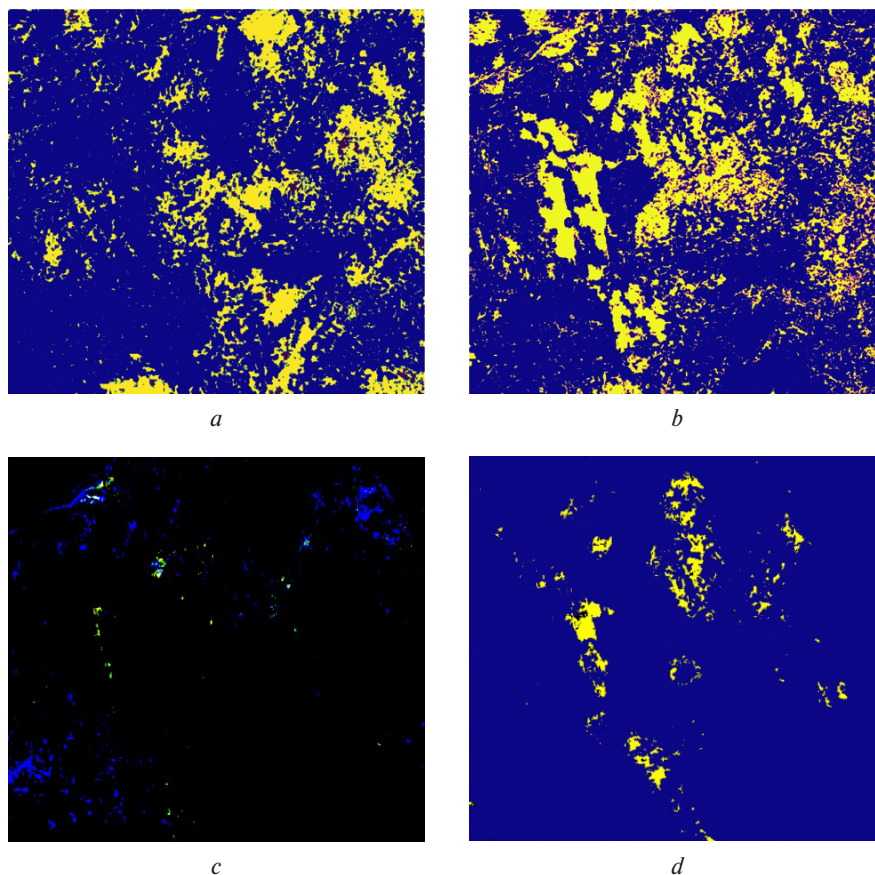
Further research included a comparison of land cover change maps, including analysis of the NDVI (Normalized Difference Vegetation Index) and NDBI (Normalized Difference Built-up Index) indicators, the method for subtracting pixel values (image differencing), and the proposed approach based on the analysis of the symmetric difference of sets of changed pixels obtained after neural network classification. The main task was to evaluate the ability of each model to accurately identify changes in the land cover, in particular, to determine the amber wash in areas characterized by a high level of dynamic changes.

A visual analysis of the maps (Fig. 3) revealed specific features of each approach used. The NDVI Changes map (Fig. 3, *a*) did not always meet expectations: instead of indicating vegetation degradation, the purple zones showed false or mixed areas. In particular, in some areas where the amber washing conditions predicted a decrease in vegetation cover due to soil removal

and the formation of ponds, NDVI showed areas of growth, which may indicate the emergence of new vegetation (e. g., algae or mosaic regeneration).

The NDBI Changes map (Fig. 3, *b*), although traditionally used to analyze built-up areas, in this study showed that the yellow areas, which were supposed to reflect newly formed open areas, partially correlated with the area of natural cover loss. However, the purple areas, which indicate areas with no changes, do not always correspond to the actual data. The method for subtracting pixel values (image differencing) summarized the general differences between the 2017 and 2023 images, which made it possible to assess trends in photosynthetically active biomass. However, this approach also revealed false-positive signals caused by natural seasonal fluctuations that are not directly related to the amber-washing process. The most informative was the proposed approach based on analyzing the symmetric difference of the set of changed pixels after neural network classification, as determined by formulas (1–3). This method made it possible to more accurately identify areas with active amber washing, providing a clear delineation of areas of vegetation degradation and changes in the hydrological regime, which are critical for monitoring the impact of amber mining.

The quantitative analysis used data that included images from different periods to identify various changes associated with natural and anthropogenic factors. The primary metrics used to assess the quality of the change maps were classification accuracy, the number of missed



A legend: ■ unchanged area; ■ land cover disturbance due to hydromechanical amber mining

Fig. 3. Land cover change maps:

*a* – NDVI Changes; *b* – NDBI Changes; *c* – image differencing; *d* – proposed technology

Table 2

Quantitative metrics for assessing the quality of land cover change maps

Change map (2017–2023 years)	Classification accuracy (%)	False Negatives (%)	False Positives (%)
NDVI Changes	72.5	18.3	9.2
NDBI Changes	65.8	22.1	12.1
Image differencing	78.9	15.6	5.5
<b>Proposed IT-technology for Change Map</b>	<b>91.3</b>	<b>4.7</b>	<b>4.0</b>

changes (false negatives), and the number of false positives (Table 2).

Table 2 shows that the Proposed IT technology for Change Map demonstrates the best results among all the maps, as it has the highest classification accuracy (91.3 %) and the lowest false-negative (4.7 %) and false-positive (4.0 %) rates. It confirms its effectiveness in detecting land cover changes associated with amber washing.

**Conclusions.** An intelligent technology for detecting land cover changes due to amber mining based on Sentinel-2 optical satellite images is proposed. The technology consists of the following stages: downloading multi-temporal optical satellite images; pre-processing, including geometric and radiometric correction; detection of land cover disturbances due to amber mining based on a hybrid architecture of convolutional neural networks (CNN + EffectiveNet-Edge) and detection of changes in time based on the symmetric difference of the set of changed pixels. The proposed hybrid convolutional neural network architecture accurately classifies land cover changes, considering texture and spectral features. Integrating MBConv blocks in the EfficientNet-Edge architecture allows us to effectively evaluate satellite images' texture and spectral features to detect land cover changes caused by anthropogenic impacts.

To train and test the neural network, a specialized dataset containing multispectral optical images obtained from the Sentinel-2 satellite was created. The dataset includes multi-temporal data, allowing us to monitor land cover changes associated with amber mining effectively.

Experimental studies of land cover change monitoring were conducted based on analyzing a test set of multispectral, multi-temporal optical images of the Sentinel-2 satellite. The studied area is located between the villages of Zhdan and Rivers in the Rivne region, and the time range covers the spring period of 2017–2024 years. It allows the model to effectively study the processes occurring in high land cover variability conditions and anthropogenic impacts, including amber mining.

A comparative analysis of deep neural network architectures showed that the proposed technology based on CNN+EfficientNet-Edge demonstrates the highest performance: F1 score (92 %), accuracy (94 %), and recall (90 %). It confirms the high ability of technology to detect land cover changes accurately.

The article comprehensively analyzes land cover change maps, including visual and quantitative evaluation. In particular, a comparative analysis of the maps

obtained by the NDVI and NDBI methods, the method for subtracting pixel values, as well as the proposed algorithm based on the study of the symmetric difference of the sets of changed pixels obtained as a result of neural network classification was carried out. The analysis results showed that the proposed algorithm provided the highest accuracy of land cover change classification (91.3 %). This algorithm made it possible to identify areas of active hydromechanical amber mining with high accuracy and clearly delineate areas of vegetation degradation and changes in the hydrological regime, which is vital for monitoring the impact of amber mining.

#### References.

- Clare, M., Piggott, M., & Cotter, C. (2021). *Assessing erosion and flood risk in the coastal zone through the application of the multilevel Monte Carlo method*. <https://doi.org/10.31223/XSS30K>
- Liu, Z., Xu, J., Liu, M., Yin, Z., Liu, X., Yin, L., & Zheng, W. (2023). Remote sensing and geostatistics in urban water-resource monitoring: A review. *Marine and Freshwater Research*, 74, 747–765. <https://doi.org/10.1071/MF22167>
- Kashtan, V., & Hnatushenko, V. (2023). Deep Learning Technology for Automatic Burned Area Extraction Using Satellite High Spatial Resolution Images. *Lecture Notes in Computational Intelligence and Decision Making. Advances in Intelligent Systems and Computing*, 1246, 664–685. Springer, Cham. [https://doi.org/10.1007/978-3-031-16203-9\\_37](https://doi.org/10.1007/978-3-031-16203-9_37)
- Kato, A., Thau, D., Hudak, A. T., Meigs, G. W., & Moskal, L. M. (2020). Quantifying fire trends in boreal forests with Landsat time series and self-organized criticality. *Remote Sensing of Environment*, 237, 111525. <https://doi.org/10.1016/j.rse.2019.111525>
- Kumar Chandan (2024). *Monitoring Deforestation Using Satellite Imagery and Machine Learning*. <https://doi.org/10.13140/RG.2.2.16598.05444>
- Kashtan, V., Hnatushenko, V., & Zhir, S. (2021). Information Technology Analysis of Satellite Data for Land Irrigation Monitoring. *2021 IEEE International Conference on Information and Telecommunication Technologies and Radio Electronics (UkrMiCo)*, Kyiv, Ukraine, (pp. 12–15). <https://doi.org/10.1109/UkrMiCo52950.2021.9716592>
- Hnatushenko, V., Kogut, P., & Uvarov, M. (2020). On Flexible Co-Registration of Optical and SAR Satellite Images. *Lecture Notes in Computational Intelligence and Decision Making. ISDMCI 2020. Advances in Intelligent Systems and Computing*, 1246, (pp. 515–534). Springer, Cham. [https://doi.org/10.1007/978-3-030-54215-3\\_33](https://doi.org/10.1007/978-3-030-54215-3_33)
- Kamarudin, M., Gidado, K., Toriman, M., Juahir, H., Umar, R., Abd Wahab, N., ..., & Maulud, K. (2018). Classification of Land Use/land Cover Changes Using GIS and Remote Sensing Technique in Lake Kenyir Basin, Terengganu, Malaysia. *International Journal of Engineering & Technology* 7, 12–15. <https://doi.org/10.14419/ijet.v7i3.14.16854>
- Pomente, A., Picchiani, M., & Del Frate, F. (2018). Sentinel-2 Change Detection Based on Deep Features. *2018 IEEE International Geoscience and Remote Sensing Symposium*, Valencia, Spain, July 22–27, (pp. 6859–6862). <https://doi.org/10.1109/IGARSS.2018.8519195>
- Fan, J., Lin, K., & Han, M. (2019). A Novel Joint Change Detection Approach Based on Weight-Clustering Sparse Autoencoders. *IEEE Journal of Selected Topics in Applied Earth Observations and Remote Sensing*, 12(2), 685–699. <https://doi.org/10.1109/JSTARS.4609443>
- Kou, J., Zhan, T., Zhou, D., Xie, Y., Da, Z., & Gong, M. (2023). Visual Attention-Based Siamese CNN with Softmaxfocal Loss for Laser-Induced Damage Change Detection of Optical Elements. *Neurocomputing*, 517, 173–187. <https://doi.org/10.1016/j.neucom.2022.10.074>
- Marsocci, V., Coletta, V., Ravanelli, R., Scardapane, S., & Crespi, M. (2023). Inferring 3D Change Detection From Bitemporal Optical Images. *ISPRS Journal of Photogrammetry and Remote Sensing*, 196, 325–339. <https://doi.org/10.1016/j.isprsjprs.2022.12.009>
- Wei, W., Ye, Y., Chen, G., Zhao, Y., Yang, X., Zhang, L., & Zhang, Y. (2025). SAR remote sensing image segmentation based on feature enhancement. *Neural New*, 185, 107190. <https://doi.org/10.1016/j.neunet.2025.107190>
- Garnot, V. S. F., & Landrieu, L. (2021). Panoptic segmentation of satellite image time series with convolutional temporal attention networks. *Proceedings of the IEEE/CVF International Conference on Computer Vision (ICCV)*, 4872–4881. <https://doi.org/10.48550/arXiv.2107.07933>

15. Shu, Y., Li, W., Yang, M., Cheng, P., & Han, S. (2021). Patch-Based Change Detection Method for Sar Images with Label Updating Strategy. *Remote Sensing*, 13(7), 1236. <https://doi.org/10.3390/rs13071236>
16. Han, Y., Javed, A., Jung, S., & Liu, S. (2020). Object-Based Change Detection of Very High Resolution Images by Fusing Pixel-Based Change Detection Results Using Weighted Dempster–shafer Theory. *Remote Sensing*, 12(6), 983. <https://doi.org/10.3390/rs12060983>
17. Jing, R., Liu, S., Gong, Z., Wang, Z., Guan, H., Gautam, A., & Zhao, W. (2020). Object-Based Change Detection for Very High-Resolution Remote Sensing Images Based on a Trisiamese-LSTM. *International Journal of Remote Sensing*, 41(16), 6209–6231. <https://doi.org/10.1080/01431161.2020.1734253>
18. Chen, P., Li, C., Zhang, B., Chen, Z., Yang, X., Lu, K., & Zhuang, L. (2022). A Region-Based Feature Fusion Network for Vhr Image Change Detection. *Remote Sensing*, 14(21), 5577. <https://doi.org/10.3390/rs14215577>
19. Myroniuk, V., Bilous, A., Khan, Y., Terentiev, A., Kravets, P., Kovalevskiy, S., & See, L. (2020). Tracking Rates of Forest Disturbance and Associated Carbon Loss in Areas of Illegal Amber Mining in Ukraine Using Landsat Time Series. *Remote Sensing*, 12, 2235. <https://doi.org/10.3390/rs12142235>
20. Zayachkivska, B., & Paliy, A. (2024). Remote monitoring of lands, the soil cover of which is disturbed due to arbitrary amber mining. *Zemleustrii, kadastr i monitoring zemel*. <https://doi.org/10.31548/zemleustriy2024.02.012>
21. Shevchuk, R. (2018). Technique for Satellite Monitoring of Illegal Amber Mining Territories Based on Integrated Landsat and Sentinel Data Processing. *Journals of Georgian Geophysical Society*, 21(1), 26–33.
22. Hnatushenko, V., Mozgovyi, D., Vasyliiev, V., & Kavats, O. (2017). Satellite Monitoring of Consequences of Illegal Extraction of Amber in Ukraine. *Naukovyi Visnyk Natsionalnoho Hirnychoho Universytetu*, 2(158), 99–105.
23. Zhang, C., Feng, Y., Hu, L., Tapete, D., Pan, L., Liang, Z., Cigna, F., & Yue, P. (2022). A Domain Adaptation Neural Network for Change Detection with Heterogeneous Optical and SAR Remote Sensing Images. *International Journal of Applied Earth Observation and Geoinformation*, 109, 102769. <https://doi.org/10.1016/j.jag.2022.102769>
24. Song, A., & Choi, J. (2020). Fully Convolutional Networks with Multiscale 3D Filters and Transfer Learning for Change Detection in High Spatial Resolution Satellite Images. *Remote Sensing*, 12, 799. <https://doi.org/10.3390/rs12050799>
25. Cui, B., Zhang, Y., Yan, L., Wei, J., & Wu, H. (2019). An Unsupervised SAR Change Detection Method Based on Stochastic Subspace Ensemble Learning. *Remote Sensing*, 11, 1314. <https://doi.org/10.3390/rs11111314>
26. Wang, G., Li, B., Zhang, T., & Zhang, S. (2022). A Network Combining a Transformer and a Convolutional Neural Network for Remote Sensing Image Change Detection. *Remote Sensing*, 14(9), 2228. <https://doi.org/10.3390/rs14092228>
27. Feng, Y., Jiang, J., Xu, H., & Zheng, J. (2023). Change Detection on Remote Sensing Images Using Dual-Branch Multilevel Intertemporal Network. *IEEE Transactions on Geoscience and Remote Sensing*, 61, 1–15. <https://doi.org/10.1109/TGRS.2023.3241257>
28. Sun, Y., Lei, L., Li, Z., & Kuang, G. (2024). Similarity and Dissimilarity Relationships Based Graphs for Multimodal Change Detection. *ISPRS Journal of Photogrammetry and Remote Sensing*, 208, 70–88. <https://doi.org/10.1016/j.isprsjprs.2024.01.002>
29. Deng, Z., Hu, S., Yin, S., Wang, Y., Basu, A., & Cheng, I. (2022). Multi-step implicit Adams predictor-corrector network for fire detection. *IET Image Process*, 16, 2338–2350. <https://doi.org/10.1049/ipr2.12491>

## Інтелектуальна технологія моніторингу земного покриття внаслідок видобутку бурштину на оптичних супутникових знімках

В. Ю. Каштан, В. В. Гнатушенко\*

Національний технічний університет «Дніпровська політехніка», м. Дніпро, Україна

\* Автор-кореспондент e-mail: [vygnat@ukr.net](mailto:vygnat@ukr.net)

**Мета.** Розробка інтелектуальної технології визначення змін земного покриття внаслідок видобутку бурштину на основі оптичних супутникових знімків Sentinel-2.

**Методика.** Представлена інтелектуальна технологія поєднує методи геометричної та радіометричної корекції, алгоритм Dark Object Subtraction, гібридну архітектуру згорткових нейронних мереж (CNN + EfficientNet-Edge), а також алгоритм виявлення змін у часі на основі симетричної різниці змінених пікселів, що забезпечує високу точність і ефективність у процесі аналізу змін земного покриття.

**Результати.** Ефективність запропонованої технології була оцінена за допомогою метрик F1-міри, відгук (Recall), точності (Precision) і загальної точності (Accuracy). Значення метрик повноти та F1-міри (92 %) підтверджують здатність системи до точного виявлення меж зон порушень земного покриття. Крім того, точність (94 %), відгук (90 %) і загальна точність (93 %) підтверджують здатність моделі ефективно класифікувати як ділянки, що зазнали впливу видобутку, так і ділянки без ознак антропогенного втручання, з мінімальною кількістю помилок. Низьке значення похибки сегментації змін земного покриття (4,7 %) свідчить про високу якість просторової інтерпретації результатів.

**Наукова новизна.** У роботі запропоноване використання згорткових нейронних мереж з архітектурою EfficientNet-Edge для визначення змін земного покриття внаслідок видобування бурштину. Цей підхід дозволяє подолати обмеження традиційних нейронних мереж прямого поширення, пов'язаних із проблемами некоректної ініціалізації й неоптимальним розподілом вагових коефіцієнтів. Зокрема, запропоноване комплексне застосування двох рівнів обробки ознак: на першому обробляються прості текстурні ознаки, що отримуються за допомогою середнього пулінгу в архітектурі CNN, на другому – спектральні ознаки, що формуються з 4D тензора на останньому згортковому шарі EfficientNet-Edge. Це дозволяє подолати нестабільність процесу навчання й підвищити здатність моделі точно виявляти зміни земного покриття, спричинені гідромеханічним видобутком бурштину. Розроблена анотація ділянок внаслідок видобутку бурштину і ділянок без ознак антропогенного втручання.

**Практична значимість.** Розроблена технологія має практичну цінність для визначення змін земного покриття, спричинених гідромеханічним видобутком бурштину. Отримані результати дають можливість ефективно оцінювати масштаби змін і сприяють прийняттю обґрунтованих управлінських рішень у сфері охорони довкілля.

**Ключові слова:** карта змін земного покриття, спектральні ознаки, текстурні ознаки, EfficientNet-Edge, глибоке навчання, згорткові нейронні мережі, оптичні супутникові знімки

*The manuscript was submitted 11.01.25.*